ELSEVIER

Polymer 40 (1998) 47–52

polymer

Tensile drawing of ethylene/vinyl-alcohol copolymers: 3. Biaxial orientation

Roland Séguéla[a,*], Karina Djezzar[a], Laurence Penel[a], Jean-Marc Lefebvre[a], Yves Germain[b]

[a]*Laboratoire 'Structure et Propriétés de l'Etat Solide', URA CNRS 234, Université des Sciences et Technologies de Lille, Bât. C6, 59655, Villeneuve d'Ascq Cédex, France*
[b]*Centre d'Etudes 'Recherche et Développement', ELF-ATOCHEM, 27470 Serquigny, France*

Received 4 December 1997; revised 30 January 1998; accepted 5 March 1998

Abstract

The phenomenological and structural aspects of biaxial drawing of a vinyl alcohol-rich ethylene/vinyl-alcohol copolymer is studied as a function of temperature. For draw temperature above the crystalline mechanical relaxation, T_α, sharp necks accompanied with catastrophic fissures develop during simultaneous biaxial drawing as well as in the first step of sequential biaxial drawing. For draw temperature below T_α, simultaneous biaxial drawing can be successfully achieved via propagation of diffuse necking so that a minimum macroscopic draw ratio of about 3 × 3 is required to obtain a uniform plastic strain. The strong interaction anisotropy of the sheet-like structure of the monoclinic phase is responsible for the fissuring trend at $T > T_\alpha$. In contrast, the isotropic mesomorphic phase that is strain-induced at $T < T_\alpha$ enables simultaneous biaxial drawing. The development of a planar texture suggests that the transformation results from transverse crystal slip. However, the random distribution of the H-bonds in the mesomorphic phase is rather consistent with an accumulation process of conformational defects that remain frozen in the crystal. © 1998 Elsevier Science Ltd. All rights reserved.

Keywords: Ethylene/vinyl-alcohol copolymer; Biaxial drawing; Mesomorphic structure

1. Introduction

Poly(vinyl alcohol) and vinyl alcohol-rich copolymers with ethylene are highly efficient gas barrier polymers. For that reason, they have great potential for applications into films for food packaging. However, they display very poor ability for bi-axial drawing that is a common processing technique to improve packaging film properties. Such materials have indeed a high propensity for fibrillation that has been attributed to a high orientation-induced crystallization rate during the first stage of drawing that is detrimental to the second-stage drawing [1]. However, it has been reported that 3 × 3 biaxial drawing can be performed simultaneously in the drawing temperature range 80°C $< T <$ 100°C, that is well below the melting point [2]. Sequential bi-axial orientation may also be achieved owing to more severe conditions, i.e. 60°C $< T <$ 80°C.

In a study of the uniaxial drawing of ethylene/vinyl-alcohol copolymers (EVOH) [3–5], we have concluded that the sheet-like structure which results from the planar distribution of the intermolecular hydrogen bonds in the stable monoclinic crystalline form involves a strong mechanical anisotropy that is responsible for a splitting trend and prejudices biaxial drawing. We have shown yet that drawing below 100°C involves a modification of the crystalline structure from monoclinic to mesomorphic with randomization of the hydrogen bond distribution about the chain axis. This strain-induced phase change benefits drawability owing to the mechanical isotropy of the mesomorphic phase. We have shown elsewhere that the screening of hydroxyl interactions by a complexing agent such as iodine is another route to disturb the sheet-like structure through the disruption of interchain hydrogen bonding. This results in an efficient means of biaxial drawing improvement [6].

2. Experimental

The ethylene/vinyl-alcohol copolymer, SOARNOL A from Nippon Gohsei, has an ethylene molar concentration of 0.44 and a weight fraction crystallinity of 0.60, as assessed from the melting enthalpy. Additional characteristics are given elsewhere [3,4]. The material was melt-cast

---

[*] Corresponding author.

0032-3861/98/$ - see front matter © 1998 Elsevier Science Ltd. All rights reserved
PII: S0032-3861(98)00219-5

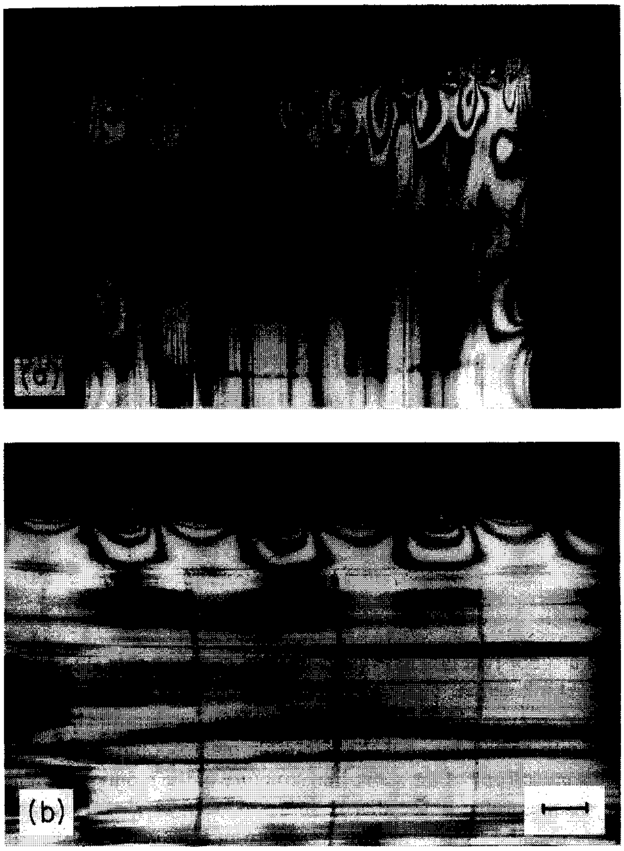

Fig. 1. Photographs between crossed polars of an EVOH sample drawn at 75°C up to $\Lambda_1 = 3.5$ at constant width: (a) end view; (b) lateral view (scale bar = 1 cm)

into films about 200 μm thick from a T-die extruder at 210°C and cooled down on a chill roll at a temperature of 90°C.

Biaxial drawing experiments have been carried out on a prototype Cellier tenter which consisted of four pantographs equipped with 10 pneumatic grips each. Two of the pantographs were moved by hydraulic jacks at right angle. The sample gauge dimensions were 100 mm × 100 mm. The drawing experiments were conducted at constant jack speed of 600 mm/min, for two different temperatures of 75° and 120°C. The actual plastic strains of the samples were determined from a square grid of 1 cm × 1 cm mesh size printed on the sample prior to drawing.

Differential scanning calorimetry (d.s.c.) measurements were carried out on Perkin-Elmer DCS-7-Delta apparatus. The heating rate was 10°C/min and the sample weight was about 5 mg. Calibration of the temperature and the heat flow scales at the same heating rate was achieved with the melting scans of high purity indium and zinc samples. The weight fraction crystallinity was calculated from the ratio of the enthalpy of fusion of the sample to that of an infinitely large perfect crystal of the copolymer, i.e. $\Delta H_f^\circ = 117 \pm 3$ J/g [3,4].

Wide-angle (w.a.x.s.) and small-angle X-ray scattering (s.a.x.s.) patterns were recorded on a Luzzati-Baro goniometer as previously described [5]. The w.a.x.s. reflexions of the monoclinic lattice have been indexed by setting the c-axis parallel to the chain axis, according to the previous study [5].

3. Results and discussion

3.1. Drawing behaviour

In this work, simultaneous biaxial drawing has been carried out successfully in a similar temperature range for which diffuse necking has been observed under uniaxial drawing, i.e. below the temperature of the α crystalline mechanical relaxation $T_\alpha \approx 110$°C [4]. The macroscopic strain should however exceed the natural draw ratio of the incipient neck in order to result in a homogeneous deformation over the whole sample. For instance, an equibiaxial macroscopic strain $\Lambda_1 \times \Lambda_2 = 3 \times 3$ at 75°C provides an almost uniformly deformed film in both directions, the natural draw ratio under uniaxial drawing being $\lambda \approx 3$ at this temperature.

Sequential biaxial drawing should be theoretically feasible at $T < T_\alpha$. After a first-step draw at 75°C up to $\Lambda_1 = 3.5$ at constant width, i.e. $\Lambda_2 = 1$, the EVOH film displays a homogeneous deformation as judged from the size of the mesh grid on the photograph of Fig. 1. The actual strain is close to $\lambda_1 = 3.5$ in the draw direction and $\lambda_2 = 0.85$ in the transverse direction due to the slight contraction of the sample that is allowed between the lateral grips as they gradually separate from each other. The interference fringes about the grip loci along the sample reveal that there are yet strong internal stress concentration and local thickness gradients due to the increasing spacing between the grips as the pantographs are stretched. At the onset of the second-step draw, these weakened regions are responsible for early crack initiation leading to the breakdown of the film sample along the grip line without significant plastic deformation in the transverse direction. This is not a material disability but a technical handicap from the tentering frame that is not encountered in the industrial process of sequential biaxial drawing.

For the draw temperature $T_d = 115$°C, the EVOH displays sharp necks that propagate all along the sample length during the first-step drawing. Fig. 2 shows that, at $\Lambda_1 = 2.8$, the actual deformation is highly heterogeneous, in contrast to the previous case. Axial cracks grow within the necked regions due to the normal tensile stress component in the sample plane. Such cracks prohibit second-step drawing in the transverse direction. This phenomenon is an intrinsic weakness of the material that has been already discussed in the previous paper regarding uniaxial drawing [4]. The sheet-like structure of the monoclinic stable crystalline form has a great propensity for predominent crystal slip parallel to the sheet planes followed by crystal splitting. This is mainly due to the collapse of the van der Waals interactions

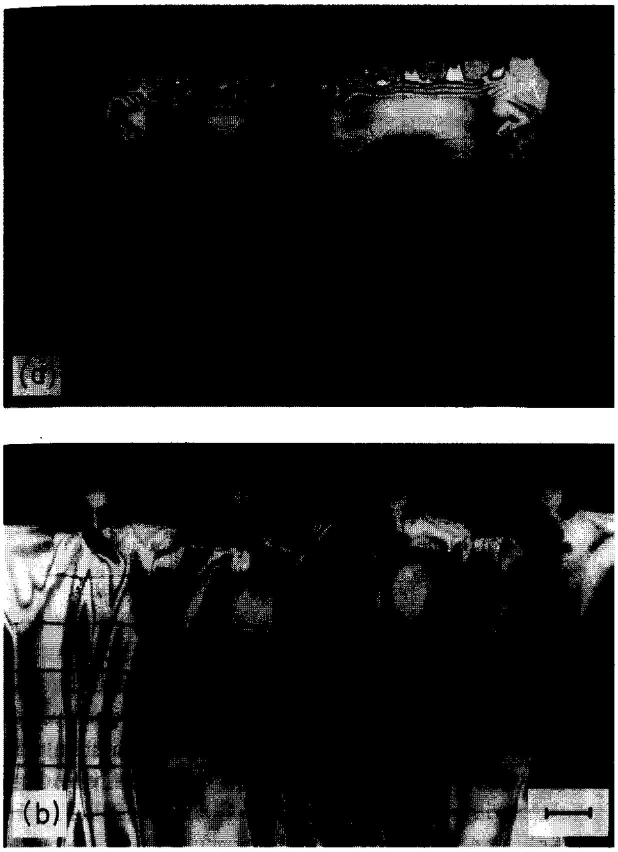

Fig. 2. Photographs between crossed polars of an EVOH sample drawn at 115°C up to $\Lambda_1 = 2.8$ at constant width: (a) end view; (b) lateral view (scale bar = 1 cm)

between the hydrogen-bonded sheets at temperature above 110°C. The crystal splitting trend turns into macroscopic fissures through the material which prohibit both simultaneous and sequential biaxial drawing.

3.2. X-ray characterization

Fig. 3*a* and *b* show the edge-view w.a.x.s. patterns recorded from EVOH uniaxially drawn at constant width, i.e. $\lambda_1 \times \lambda_2 = 3.5 \times 0.85$, with the X-ray beam parallel to the draw axis, for 115° and 75°C. For the higher temperature, the sample is taken from a local necked region in the heterogeneously drawn film. Nearly random orientation of the crystalline structure is observed for both temperatures. The slight unevenness of the Debye–Scherrer rings is due to the sample preparation consisting of 12 piled film pieces whose surface is not perfectly parallel to the incident beam. There is no trend for planar texture despite the planar strain deformation state in either case.

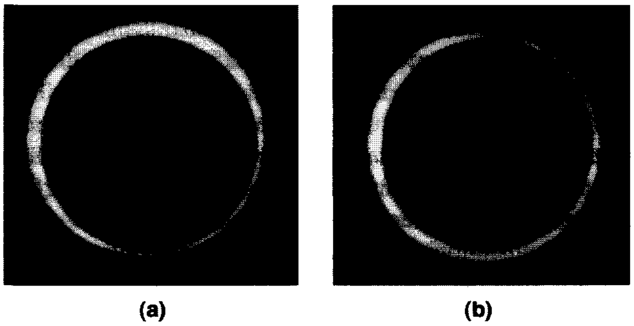

(a) (b)

Fig. 3. Edge-view w.a.x.s. patterns of EVOH samples drawn at $\lambda_1 \times \lambda_2 = 3.5 \times 0.85$, for (a) $T_d = 115$°C and (b) $T_d = 75$°C (X-ray beam parallel to the draw axis)

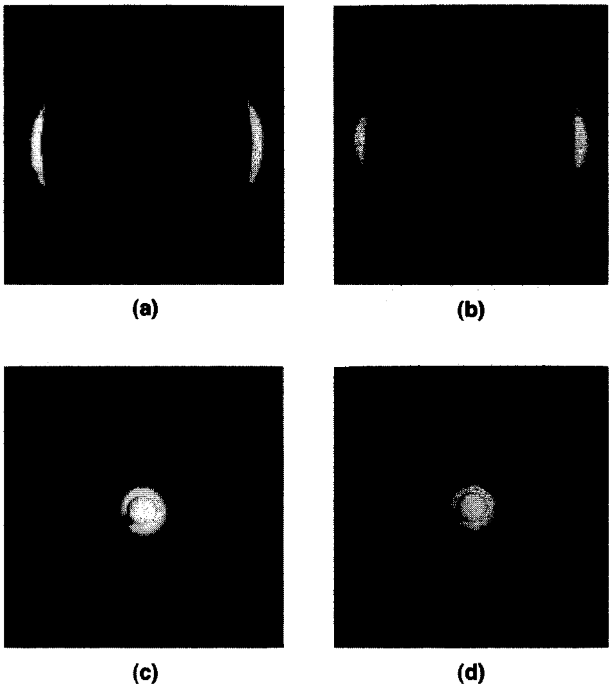

(a) (b)

(c) (d)

Fig. 4. Through-view w.a.x.s. and s.a.x.s. patterns of EVOH samples drawn at $\lambda_1 \times \lambda_2 = 3.5 \times 0.85$: w.a.x.s. for (a) $T_d = 115$°C and (b) $T_d = 75$°C; s.a.x.s. for (c) $T_d = 115$°C and (d) $T_d = 75$°C (draw axis vertical)

The through-view w.a.x.s. patterns of Fig. 4*a* and *b* reveal the structural orientation parallel to the draw axis, for both temperatures. Moreover, despite the broadness of the equatorial diffraction arcs, these patterns show that the monoclinic structure is preserved at 115°C, whereas a mesomorphic structure develops for 75°C. The s.a.x.s. patterns of Fig. 4*c* and *d* corroborate this conclusion, as the loss of long period scattering (Fig. 4*d*) has been shown to be a characteristic feature of the mesomorphic phase due to a very low electronic density contrast with the amorphous phase [5].

The strain-induced phase change from the monoclinic to the mesomorphic structure has been ascribed a prime role in the improved drawability of EVOH at low temperature thanks to the random distribution of the hydrogen (H) bonds about the chain axis that makes the new crystal lattice mechanically isotropic [3,4]. The occurrence of this phase change during the first-step drawing at 75°C provides a homogeneous deformation of the samples without crack initiation that allows transverse redrawing. In contrast, the sheet-like structure of the monoclinic crystalline phase

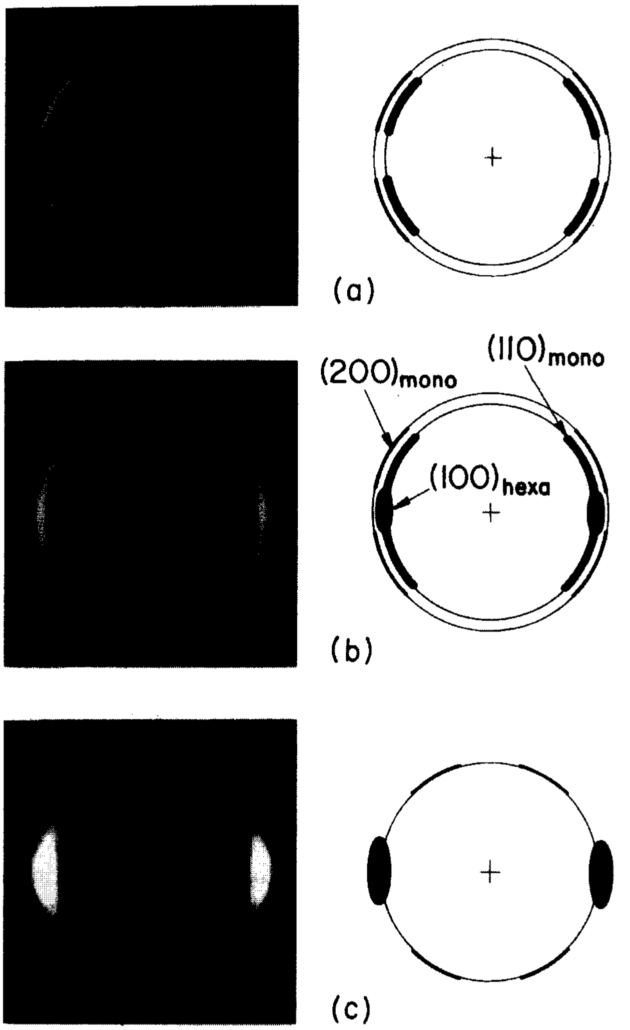

Fig. 5. Edge-view w.a.x.s. patterns of EVOH samples biaxially drawn at $T_d = 75°C$: (a) $\lambda_1 \times \lambda_2 = 1.5 \times 1.5$; (b) $\lambda_1 \times \lambda_2 = 2.2 \times 2.2$; (c) $\lambda_1 \times \lambda_2 = 3.3 \times 3.3$ (film plane vertical)

involves a natural propensity for fissure initiation at the microscopic scale due to the strong anisotropy of chain interactions within and between the H-bonded sheets that favours crystal splitting.

The achievement of simultaneous biaxial drawing without crack formation at 75°C is an additional piece of evidence of the major role of the mesomorphic structure. Edge-view w.a.x.s. patterns taken at three stages of the drawing process are reported in Fig. 5. At $\lambda_1 \times \lambda_2 = 1.5 \times 1.5$ (Fig. 5*a*), the quadrant position of the (110) and (200) nodes reveals a preferential crystalline orientation of the corresponding crystallographic planes slightly tilted with respect to the film surface. This seems to be an intermediate step toward a double planar texture similar to that often reported for biaxially drawn polyethylene [7–10]. Besides its transitory character, the tilt of the main crystallographic planes makes them able to experience a close-to-maximum resolved shear stress for either longitudial or transverse crystal slip. The driving force to the oblique orientation certainly relies on a lower energy path for plastic deformation. It is to be stressed that the similar orientational trend of the (110) and (200) planes is quite different from the double planar texture of polyethylene which undergoes sequential biaxial drawing. At the stage $\lambda_1 \times \lambda_2 = 2.2 \times 2.2$ (Fig. 5*b*), partial phase change occurs with a concomitant orientation of the main crystallographic plane of the new phase parallel to the film surface. It is worth noticing that the different orientation of the new mesomorphic structure (equatorial diffraction) with respect to that of the mother monoclinic structure (quadrant diffraction) makes more clear the phase transformation onset, compared to the case of uniaxial drawing [4]. In the latter case, the (200) reflexion very soon shifts to the equatorial position while the (110) reflexion takes a quadrant position before to gradually shift toward the equator. So, one can hardly distinguish the early stage of the appearance of the unique mesomorphic reflexion on the equator from that of the parent monoclinic structure. At the draw stage $\lambda_1 \times \lambda_2 = 3.3 \times 3.3$ (Fig. 5*c*), the whole crystalline structure has turned into mesomorphic form with its main crystallographic plane parallel to the film surface. The four additional weaker reflexions in quadrant positions are consistent with the hexagonal symmetry proposed for the mesomorphic structure [5]. The six reflexions thus correspond to the three equivalent {100} planes. They are besides relevant to a planar texture that is a common feature to various kinds of biaxially drawn semi-crystalline polymers such as polyethylene [7–10], polypropylene [11] and polyethylene terephthalate [12].

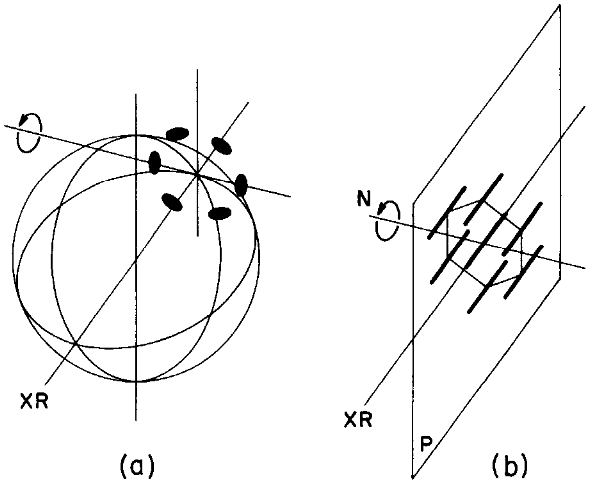

Fig. 6. Schematic pictures of (a) the reciprocal lattice and reflexion sphere corresponding to (b) the planar texture of the direct hexagonal lattice (P is the plane of the biaxially oriented film, N is the film normal and XR is the X-ray incident beam)

Worth mentioning is the fact that the through-view w.a.x.s. patterns display isotropic distribution of crystal orientation about the film normal for the three drawing stages studied above. This is a general behaviour for simultaneous equibiaxial drawing [7–12]. However, it has been reported that sequential equibiaxial drawing involves a

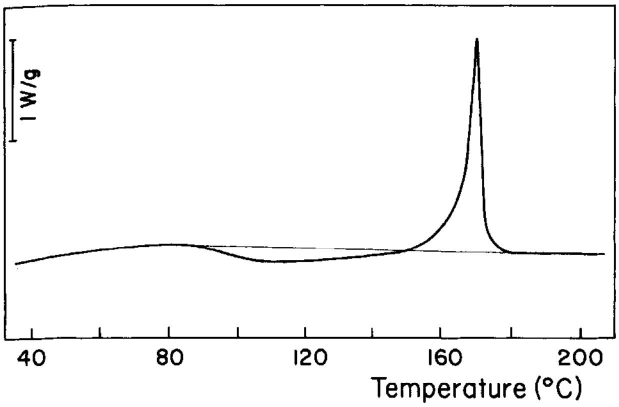

Fig. 7. D.s.c. heating curve of an EVOH sample biaxially drawn at $\lambda_1 \times \lambda_2 = 3.3 \times 3.3$, at $T_d = 75°C$

preferred orientation of the crystal chains in the direction of the second step draw [12,13]. It seems that, in spite of macroscopic equivalence, simultaneous sequential biaxial drawing processes do not follow the same deformation pathway at a microscopic scale which results in a different crystalline texture. This is likely to involve significant differences in the mechanical properties.

The occurrence of the main mesomorphic reflexion in the equatorial position (Fig. 5*c*) deserves some comment. A perfect planar texture with a preferred orientation of the (100) crystallographic plane of the hexagonal structure parallel to the film surface would result in no scattering due to razing incidence. Fig. 6 is a schematic picture of the hexagonal planar texture and the reciprocal lattice with the reflexion sphere. The two equatorial nodes of the reciprocal lattice corresponding to the (100) planes parallel to the film surface are out of the scattering position, nevertheless a good deal of them may actually scatter thanks to chain orientation fluctuations about the film plane that strongly broadens the node size. As a matter of fact, the azimuthal dispersion of the (100) reflexion that can be roughly estimated to $\Delta\phi \approx \pm 15°$ indicates a significant fluctuation of the chain orientation about the film plane so that a good deal of mesomorphic crystals may lie at the proper scattering incidence. By comparison, the tilt angle of the film normal necessary to bring the (100)* reciprocal node into reflexion is equal to the Bragg incidence, i.e. $\theta \approx 10°$ [4]. In contrast, the four quadrant (100)* nodes of the reciprocal hexagonal lattice (Fig. 6*a*) have a very weak scattering intensity that results from the low probability of the crystals to stand at the Bragg incidence. Only the axial symmetry about the normal to the film plane allows a very small number of crystals to be in a scattering position and contribute to the quadrant mesomorphic diffraction.

A quite similar orientational trend in conjunction with crystal phase change has been reported in the case of polyamide 11 submitted to uniaxial planar compression which is equivalent equibiaxial drawing [14].

3.3. Thermal behaviour

The d.s.c. thermogram of Fig. 7 is the heating curve of a copolymer A sample biaxially drawn at $\lambda_1 \times \lambda_2 = 3.3 \times 3.3$, for $T_d = 75°C$. The exotherm that spans the temperature range 90–140°C is roughly similar to that observed for uniaxially drawn samples [5] and is relevant to the transformation of the strain-induced mesomorphic phase into stable monoclinic crystals during the heating scan. However, in the present case of biaxial drawing, the exotherm onset is about 20° below that observed in the case of uniaxial drawing at $\lambda = 4$. Moreover, the transformation enthalpy of −28 J/g is much greater than the higher value measured in the case of uniaxial drawing, i.e. −10 J/g [5]. Considering that the mesomorphic structure is stable up to 110°C, it seems that some recrystallization of severely distorted crystals contributes an additional exothermal effect.

3.4. Mechanism of phase change

Crystal phase change in polyethylene is a well-known phenomenon that is usually ascribed to coherent transverse slip [15–17]. Indeed, such a mechanism enables modification of the molecular arrangement in the basal plane of the crystal lattice. The fact that phase change takes place after a significant amount of plastic strain is reached in the present study, namely about $\lambda_1 \times \lambda_2 = 2.2 \times 2.2$ in simultaneous biaxial drawing, suggests the requirement of a stress level higher than the yield stress. This is consistent with a greater critical shear stress for transverse slip than that of chain slip which is the main process of yielding since the Burgers vector of chain slip is shorter than that of transverse slip. Besides, the oblique preferred orientation of the [001] chain axis of the monoclinic structure that is observed within the sample thickness at the onset of phase change (Fig. 5*b*) necessarily involves that the crystals being in longitudinal slip position with respect to one of the two principal tensile stresses are in favourable transverse slip position with respect to the other one, i.e. the resolved shear stress is optimum. In support of the above statement, it is worth noticing Gerrits and Young's studies of polyethylene submitted to either simultaneous biaxial or uniaxial planar orientation [10,18]: the crystallographic analysis of the build up of a double planar texture in both cases was assigned to the occurence of transverse crystal slip. In the present case of EVOH, such a double planar texture that seems to begin to form at $\lambda_1 \times \lambda_2 = 1.5 \times 1.5$ (Fig. 5*a*) does not develop further due to the phase change involving a transformation of the (110) and (200) monoclinic planes into a unique {100} plane family in the hexagonal lattice of the mesomorphic structure. Notwithstanding, a mesomorphic planar texture builds up.

In the case of EVOH uniaxial drawing [5], the occurrence of transverse slip discussed above is much less likely than for simultaneous biaxial drawing because of very weak tensile transverse stress. Besides we have observed that phase transformation can occur at 120°C, for draw ratios $\lambda > 6$ involving a strong chain orientation parallel to the draw axis that cannot allow transverse slip. So, we suspect that phase change occurs via chain slip owing to the conformational chain defects that are necessary for activation of chain slip and that remain frozen in the crystalline structure, either when drawing is performed below the α crystalline relaxation temperature or when the sample is quickly cooled below T_α after drawing at high temperature. Such a process of generation and freezing of conformational defects, randomly along the chains, is likely to afford an isotropic distribution of the H-bonds about the chain axis and to account thus for the hexagonal symmetry of the mesomorphic structure. In contrast, coherent transverse slip is not expected to disturb the H-bonded sheet structure of the monoclinic phase.

The concept of conformational defect in the all-trans chain conformation of poly(vinyl alcohol) and ethylene vinyl-alcohol copolymers has been introduced by Nakamae and co-workers [19–21] to account for the change of elastic modulus and structure with temperature and composition. In the mid-composition range, EVOH copolymers have a pseudo-hexagonal structure characterized by a conformational disorder in the chains that reduces intermolecular interactions compared with polyethylene and poly(vinyl alcohol).

The origin of conformational chain defects in the course of plastic deformation of an EVOH copolymer having a monoclinic stable structure lies in the dislocation-governed elementary mechanisms of crystal slip. Such defects associated with the α mechanical relaxation in the crystal are the grounds of chain mobility. We have discussed their primary role in the plastic behaviour of polyethylene [22]. In the present case of EVOH, conformational defects are stress-activated during drawing below T_α and remain frozen in the crystal. However, above T_α, thermal activation is sufficient to overcome the energy barrier of the conformational defects, so that the chains rearrange themselves into the more stable crystalline structure. This is consistent with the observed stability temperature limit of 110°C for the mesomorphic structure[5], that is about T_α.

4. Conclusion

The sheet-like structure of EVOH copolymers is an obstacle to biaxial orientation at temperatures close to the melting point due to its highly anisotropic character that involves a strong propensity for crack initiation and propagation. Simultaneous biaxial drawing of EVOH can be carried out at 75°C thanks to a strain-induced phase change of the stable monoclinic form into a mesomorphic state. The random distribution of the H-bonds about the chain axis is the main feature of the mesomorphic structure. It involves hexagonal symmetry and mechanical isotropy of the unit cell. Plasticity defects of conformational origin are proposed to be the grounds of the phase change. Due to the thermal activation of molecular mobilities in the crystalline phase, the α relaxation is the upper temperature limit of stability of the mesomorphic structure.

The build up of a planar texture upon biaxial drawing might result from the operation of transverse slip in the deformation process. However, it is doubtful that a coherent transverse slip could be responsible for strain-induced mesomorphic structure. There are indeed some pieces of evidence in favour of a gradual accumulation of plasticity defects during chain slip.

Acknowledgements

Financial support to this work by ELF-ATOCHEM is greatly acknowledged.

References

[1] Okaya T, Ikari K. In: Finch CA, editor. Polyvinyl Alcohol developments. New York: John Wiley, 1992, chap. 8.
[2] Masuda M. In: Finch CA, editor. Polyvinyl Alcohol Developments. New York: John Wiley, 1992, chap. 12.
[3] Djezzar K, Lefebvre JM, Séguéla R, Germain Y. Am Soc Mech Eng, Appl Mech Div 1995;203:115.
[4] Djezzar K, Penel L, Lefebvre JM, Séguéla R, Germain Y. Polymer, 1998;39:3945.
[5] Penel L, Djezzar K, Lefebvre JM, Séguéla R, Fontaine H. Polymer, in press.
[6] Séguéla R, Djezzar K, Lefebvre JM. Polymer, in press.
[7] Adams GC. J Polym Sci, Polym Phys Ed 1971;9:1235.
[8] Sakai Y, Miyasaka K. Polymer 1988;29:1608.
[9] Kyu T, Fujita K, Cho MH. Polym Eng Sci 1989;29:383.
[10] Gerrits NSJA, Young RJ. J Polym Sci, Polym Phys Ed 1991;29:825.
[11] Tanaka H, Okajima S. J Polym Sci, Polym Lett Ed 1977;15:349.
[12] Chang H, Schultz JM, Gohil RM. J Macromol Sci, Phys 1993;B32:99.
[13] Karacan I, Taraiya AK, Bower DI, Ward IM. Polymer 1993;34:2691.
[14] Autran J-P. Ph.D. thesis, University of Massachusetts, Amherst, 1990, chap. 5.
[15] Seto T, Hara T, Tanaka K. Jpn J Appl Phys 1968;7:31.
[16] Hay IL, Keller A. J Polym Sci, Polym Symp 1970;30:289.
[17] Allan P, Bevis M. Proc. R. Soc. London 1974;A351:75.
[18] Gerrits NSJA, Young RJ. J Mater Sci 1991;26:2137.
[19] Nakamae K, Kameyama M, Matsumoto T. Polym Eng Sci 1979;19:572.
[20] Nakamae K, Nishino T, Ohkubo H, Matsuzawa S, Yamaura K. Polymer 1992;33:2581.
[21] Nishino T, Takano K, Nakamae K. Polymer 1995;36:959.
[22] Séguéla R, Elkoun S, Gaucher-Miri V. J Mater Sci, 1998;33:1273.